Collective behavior of brain tumor cells: The role of hypoxia

Evgeniy Khain,[1] Mark Katakowski,[2] Scott Hopkins,[1] Alexandra Szalad,[2] Xuguang Zheng,[2] Feng Jiang,[2] and Michael Chopp[1,2]
[1]*Department of Physics, Oakland University, Rochester, Michigan 48309, USA*
[2]*Department of Neurology, Henry Ford Hospital, Detroit, Michigan 48202, USA*
(Received 2 July 2010; revised manuscript received 4 February 2011; published 29 March 2011)

We consider emergent collective behavior of a multicellular biological system. Specifically, we investigate the role of hypoxia (lack of oxygen) in migration of brain tumor cells. We performed two series of cell migration experiments. In the first set of experiments, cell migration away from a tumor spheroid was investigated. The second set of experiments was performed in a typical wound-healing geometry: Cells were placed on a substrate, a scratch was made, and cell migration into the gap was investigated. Experiments show a surprising result: Cells under normal and hypoxic conditions have migrated the same distance in the "spheroid" experiment, while in the "scratch" experiment cells under normal conditions migrated much faster than under hypoxic conditions. To explain this paradox, we formulate a discrete stochastic model for cell dynamics. The theoretical model explains our experimental observations and suggests that hypoxia decreases both the motility of cells and the strength of cell-cell adhesion. The theoretical predictions were further verified in independent experiments.

DOI: 10.1103/PhysRevE.83.031920 PACS number(s): 87.18.Gh, 87.18.Hf, 87.19.xj

I. INTRODUCTION

Collective behavior of living cells [1] is an intriguing and challenging phenomenon not only from the biological perspective, but also from the physical point of view. This explains an increasingly growing interest about this subject in the physics community [2]. A remarkable range of collective behavior is displayed in morphogenesis [3], wound healing [4], and tumor growth [1,4,5]. In the present study, we focus on the invasion of aggressive malignant brain tumors [6].

Gliomas are the most common type of primary brain tumors [7]. A hallmark of malignant gliomas is their ability to invade into surrounding brain tissue. Glioma cells not only proliferate (divide), but detach from the tumor core and actively migrate away into the extracellular matrix [4]. Therefore, surgery is commonly noncurative as cells invade the brain and escape resection [8]. The invasive nature of malignant brain tumors often leads to recurrence: formation of distant recurrent (secondary) tumors in the invasive region. Experimental observations show that cells on the surface of a primary tumor (so-called proliferative cells) divide much more frequently than individual invasive cells [8,9]. However, invasive cells might form clusters, which can eventually develop into secondary tumors.

In experiments, the growth of glioma spheroids in transparent gel has been investigated. The observed patterns are different for two cell lines; the mutant cells (U87-ΔEGFR) form small clusters within the invasive region, while the wild type cells (U87) do not cluster [10,11]. More strikingly, when cells are placed on a substrate, wild type cells remain homogeneously distributed over the system, while mutant type cells eventually form clusters, which grow with time [12]. Using discrete stochastic modeling [12,13], we have shown that radically different morphologies can result even from small differences in the strength of cell-cell adhesion. When the adhesion parameter becomes larger than its threshold value, the uniform system becomes unstable, which leads to phase separation: Clusters coexist with individual migrating cells. This idea was inspired by a very different physical phenomenon: a ferromagnetic phase transition in the Ising model [14]. Importantly, the theoretical predictions were verified in a separate experiment [12].

The main focus of the present work is on an intriguing question: How does hypoxia (lack of oxygen) affect cell behavior? Cells inside a primary brain tumor are regularly subjected to hypoxic conditions. It is well known that hypoxia leads to increased tumor invasion [15]; however, the mechanism of this phenomenon remains unclear. How do hypoxic conditions affect cell motility, cell proliferation, and cell-cell adhesion? We investigated these problems both experimentally and theoretically; we further confirmed our theoretical predictions in additional experiments.

II. EXPERIMENTS

A series of experiments were performed with cells cultured under normoxic (20 percent oxygen) and hypoxic (less than 1 percent oxygen) conditions. First, we measured the proliferation rate of normoxic and hypoxic cells. There, cells were placed uniformly on a substrate, and the cell density was measured as a function of time. In all the experiments we performed, culture wells were polystyrene, modified by incorporation of oxygen ions, producing a surface that becomes hydrophilic and negatively charged when medium was added, which enabled cell attachment and spreading. We checked that the cells remain uniformly distributed over the system and did not form clusters [12]. We fitted the experimental growth curves with the modified logistic growth formula, solving the equation

$$\frac{du}{dt} = \alpha(u)\,u, \tag{1}$$

where the rate of proliferation depends on the local area fraction (normalized cell density) $0 < u < 1$. There are many ways to model the density dependence of the proliferation rate. For example, one can consider $\alpha_1(u) = \alpha\,(1+u)^{\beta}(1-u)$. Here, $\beta = 0$ gives the usual logistic growth formula; it is known, however, that the proliferation rate is more or less constant at small and intermediate densities and decreases at high densities due to contact inhibition effect. Another

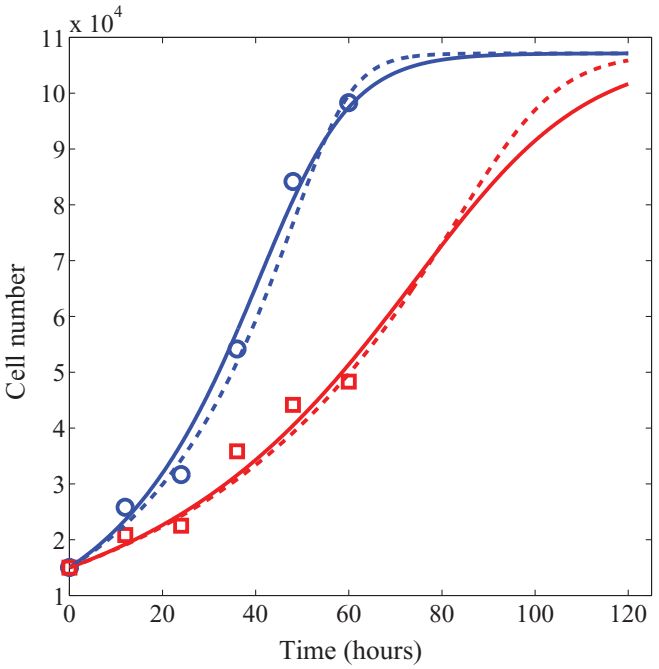

FIG. 1. (Color online) U87 glioma cell proliferation on a substrate: cell number as a function of time. Symbols show experimental results for cell proliferation under normoxic (circles) and hypoxic (squares) conditions. A theoretical fit given by Eq. (1) for the two expressions for $\alpha(u)$: $\alpha_1(u)$, $\beta = 1.73$, solid lines and $\alpha_2(u)$, $\nu = 6$, dashed lines. The parameters are $u_0 = 0.14$, $\alpha = 1/29$ hour^{-1} (upper solid line) and $\alpha = 1/53$ hour^{-1} (lower solid line); $u_0 = 0.14$, $\alpha = 1/29$ hour^{-1} (upper dashed line) and $\alpha = 1/50$ hour^{-1} (lower dashed line).

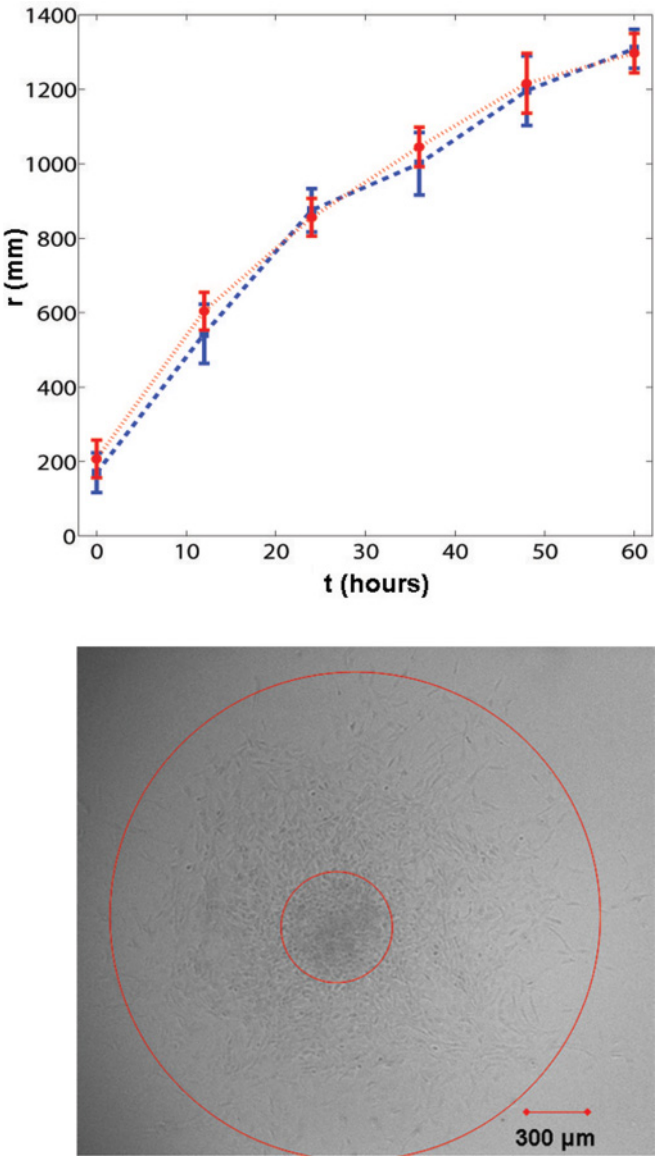

FIG. 2. (Color online) U87 glioma cell migration away from a tumor spheroid. The upper panel shows the invasive radius as a function of time for both normoxic (dashed line, squares) and hypoxic (dotted line, circles) cells; the results are averaged over 4 sets of experiments. The lower panel shows a snapshot of the system kept under hypoxic conditions (view from above) 60 hours after beginning of the experiment; the outer circle shows the borders of invasive region; the invasive radius here is approximately 1200 μm.

way to generalize the standard logistic growth is to assume $\alpha_2(u) = \alpha(1 - u^\nu)$, a well-known Richards growth function, which is widely used in biology [16]. We found that hypoxia reduces cell proliferation. For the two growth formulas, the results are almost identical: The measured proliferation rates are $\alpha_{\text{norm}} = 1/29$ hour^{-1} and $\alpha_{\text{hyp}} = 1/53$ hour^{-1} [using $\alpha_1(u)$] or $\alpha_{\text{hyp}} = 1/50$ hour^{-1} [using $\alpha_2(u)$]. The resulting growth curves are shown in Fig. 1. The computed proliferation rates were verified in an independent experiment, where cells were stained with Ki67 (a cellular marker for proliferation), and the number of proliferating cells under both normoxic and hypoxic conditions was directly counted.

Then we performed two different experiments on cell migration. In the first experiment, glioma spheroids were placed on a substrate (hereinafter "spheroid" experiment). The experiment lasted for 60 hours; cells detached from the spheroids and migrated away. We took pictures every 12 hours and measured the distance that cells migrated (invasive radius) as a function of time for both normoxic and hypoxic cells. Figure 2 shows the time dependence of the invasive radius. One can see that the overall migration of the cells in either normoxic or hypoxic conditions was similar.

The second experiment that we performed showed an opposite result! We placed cells uniformly on a plastic substrate and scratched a 2-mm-wide gap, creating a typical wound-healing geometry (hereinafter "scratch" experiment). We then followed the dynamics of the gap closure, under both normoxic and hypoxic conditions; Fig. 3 shows a representative snapshot 24 hours after the beginning of the experiment. Surprisingly, in the wound-healing assay, hypoxic cells migrated *less* then normoxic cells. Analyzing experimental images, we computed the distance that cells migrated, averaging over many sets of experiments and over the lateral coordinate. We observed that the front of normoxic cells had moved 1.02 ± 0.21 mm in 24 hours whereas the front of hypoxic cells had moved only 0.73 ± 0.14 mm. How can this paradox be explained?

The first naive attempt to attack this problem would be the following. Cell invasion is often modeled as propagation of fronts of cells that can be described by the Fisher-Kolmogorov

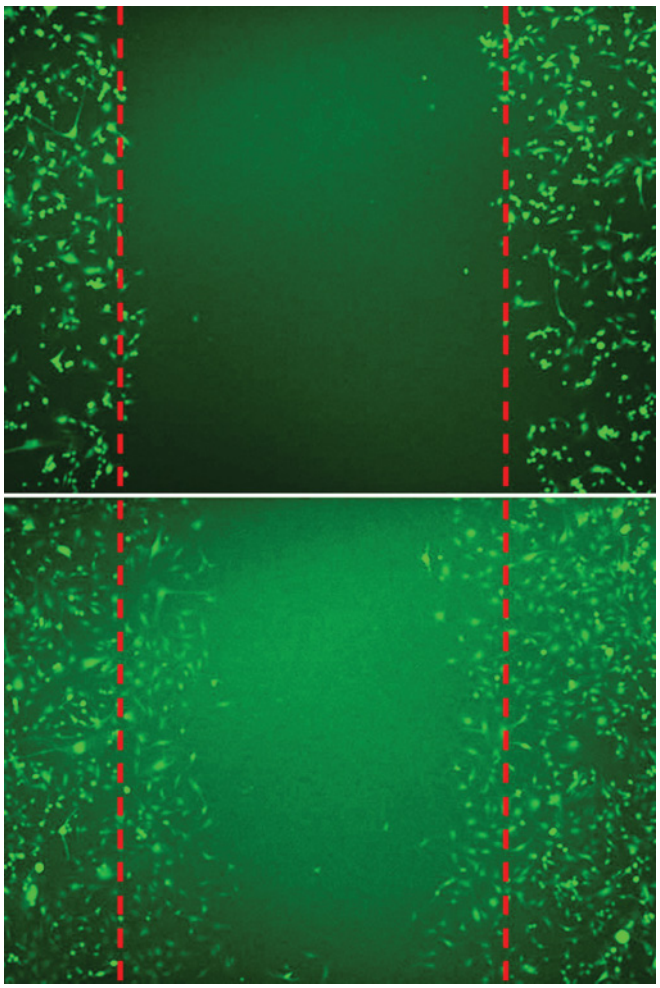

FIG. 3. (Color online) U87 glioma cell migration on a substrate: closing the scratch. Initially cells were uniformly placed on a plastic substrate, and a 2-mm-wide scratch was made (upper panel). The lower panel shows a snapshot of the system 24 hours after the beginning of the experiment, under normoxic conditions. We measured the distance that cells had migrated in 24 hours for both normoxic and hypoxic cells. Averaging over many experimental runs and over the lateral coordinate shows that normoxic cells have migrated 1.02 ± 0.21 mm, and hypoxic cells have migrated 0.73 ± 0.14 mm.

equation for the normalized local density of cells, $u(x,t)$ [4,17]:

$$\frac{\partial u}{\partial t} = D\,\frac{\partial^2 u}{\partial x^2} + \alpha\, u\,(1-u). \tag{2}$$

Here the local cell density u changes in time due to cell motility (the first term on the right hand side) and cell proliferation (the second term on the right hand side). For the constant proliferation rate α, the basic velocity of cell invasion is $v = 2\sqrt{D\alpha}$ [4,17], where D is the cell diffusion coefficient. According to the spheroid experiment, normoxic and hypoxic cells have migrated the same distance (so that the velocity of front propagation is the same for both types of cells, Fig. 2). Since normoxic cells proliferate faster than hypoxic ones, $\alpha_{\rm norm} > \alpha_{\rm hyp}$, the hypoxic cells should have larger motility (larger D). But then cells should have migrated the same distance in the scratch experiment as well. To explain this controversy, we should take into account the phenomenon of cell-cell adhesion.

III. DISCRETE STOCHASTIC MODELING

Agent-based modeling of cell migration has become increasingly popular in recent years [5,18]. Here we employ a discrete stochastic model for cell migration, introduced in [12,13]; the modeling incorporates not only cell proliferation and cell motility, but also cell-cell adhesion. The basic unit of the model is a single cell. Consider a two-dimensional square lattice (the same model can be formulated in three dimensions); each lattice site can be either empty or occupied by a single cell. The lattice distance is taken to be 20 μm, which is the effective diameter of a glioma cell. A randomly chosen cell can either proliferate to an empty neighboring site or migrate there, where the probabilities for proliferation and migration are determined from the experimentally measured rates of proliferation and migration. The probability for proliferation is given by the rate of proliferation times the characteristic diffusion time $\bar{\alpha}(n) = \alpha(u = n/4)\, t_{\rm diff}$, where the expression for $\alpha(u)$ is discussed after Eq. (1), $t_{\rm diff}$ is the average time required for a cell to move the distance equal its own diameter (this time is of the order of 10 minutes), and n is the number of the nearest neighbors (which can vary between 0 and 4). The probability for migration is $[1-\bar{\alpha}(n)](1-q)^n$, where q is the cell-cell adhesion parameter. The case $q = 0$ represents no adhesion. The probability for migration decreases as the adhesion parameter q increases, since a cell needs to detach from its neighbors. The adhesion parameter q can be experimentally measured since it is related to the shed rate of invasive cells from the tumor surface [12]. Cells with $q = 1$ will not detach from the tumor at all, so any measured shed rate corresponds to $q < 1$. After each "single cell step," the time is advanced by $t_{\rm diff}/N$, where N is the current number of cells. The model does not directly incorporate the cell-substrate (or cell-matrix) adhesion, which is an important factor in cell migration [19]; however, it is taken into account indirectly. Cell-substrate adhesion is known to affect cell migration [20]; therefore, a specific migration time $t_{\rm diff}$ corresponds to a specific strength of cell-substrate adhesion [21].

This model is now applied to describe the two main experiments we performed: (1) Cells migrate away from the spheroid and (2) cells migrate in the scratch wound geometry. The four unknown parameters of the model are the respective diffusion times and adhesion parameters for glioma cells under normoxic and hypoxic conditions: $t_{\rm diff}^{\rm norm}$, $t_{\rm diff}^{\rm hyp}$, $q_{\rm norm}$, and $q_{\rm hyp}$. The distance r that the cells have migrated depends on these parameters: $r = r(t_{\rm diff}, q)$. We performed extensive numerical simulations of the model, computing r for different sets of parameters in the two settings, keeping the proliferation rate α constant (assuming the experimentally found values for proliferation). In the scratch wound geometry, we averaged the results over many simulations and over the lateral coordinate. In the spheroid geometry, we averaged the results over many simulations and over the azimuthal direction.

Let us now plot curves $r = {\rm const}$ in the phase plane $(t_{\rm diff}, q)$, where the value of the constants is taken from experiments.

Consider, for example, the scratch experiment with cells under normoxic conditions. In the experiment, cells migrated $r = 1020$ μm in 24 hours. In the model, we choose a value of cell-cell adhesion parameter q and compute r for various diffusion times $t_{\rm diff}$. Then we find the value of $t_{\rm diff}$ for which $r = 1020$ μm. This gives a pair $(t_{\rm diff},q)$. Choosing a different value of q we get a different value of $t_{\rm diff}$. This procedure gives the curve $r = {\rm const}$ in the $(t_{\rm diff},q)$ phase plane. Figure 4 shows four such curves. The upper panel describes simulations for cells under normoxic conditions: The dotted line corresponds to the spheroid experiment (Fig. 2), $r = 1300$ μm; the solid line corresponds to the scratch experiment (Fig. 3), $r = 1020$ μm. The lower panel describes simulations for cells under hypoxic conditions: The dotted line corresponds to the spheroid experiment (Fig. 2), $r = 1300$ μm; the solid line corresponds to the scratch experiment (Fig. 3), $r = 730$ μm. Notice that the role of adhesion in the scratch wound geometry is not high: The distance r depends on q rather weakly. In the case of spheroid experiment, the role of adhesion is higher, since cells first need to detach from the spheroid.

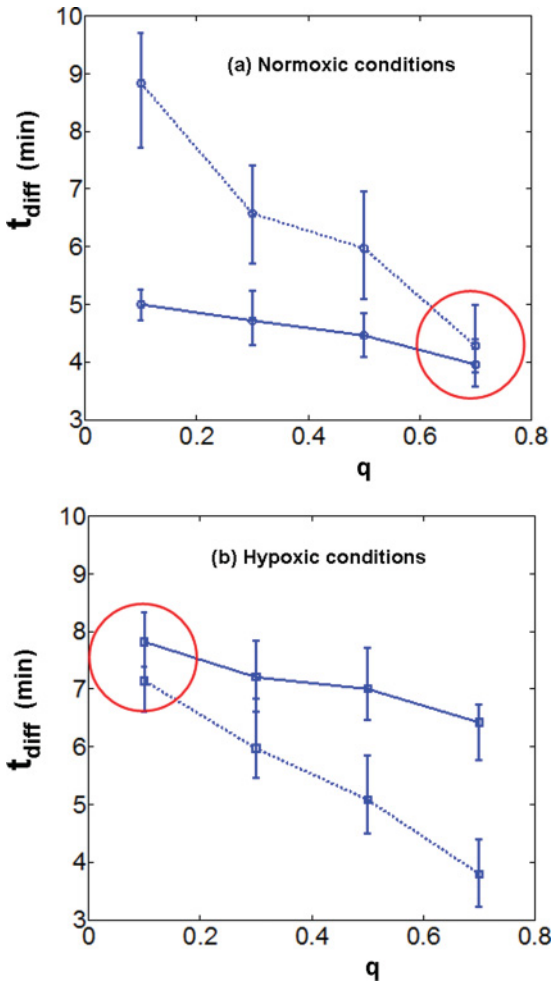

FIG. 4. (Color online) Constant distance curves $r(t_{\rm diff},q) = r_{\rm exp}$ obtained from numerical simulations of the discrete stochastic model. The distance that the cells have migrated depends on two parameters: the diffusion time $t_{\rm diff}$ and the adhesion parameter q. Shown are four constant distance curves $r = r_{\rm exp}$, which correspond to spheroid (dotted lines) and scratch (solid lines) experiments for normoxic (upper panel) and hypoxic (lower panel) cells. The region of probable intersection between the two curves in each panel (shown by circles) determines the cell parameters: $t_{\rm diff}$ and q. Comparing the two regions, one can see that $t_{\rm diff}^{\rm norm} < t_{\rm diff}^{\rm hyp}$ and $q_{\rm norm} > q_{\rm hyp}$. The experimental parameters are $r_{\rm exp} = 1.30$ mm for spheroid experiments for both normoxic and hypoxic cells (Fig. 2); for the scratch experiment (Fig. 3) $r_{\rm exp} = 1.02$ mm and $r_{\rm exp} = 0.73$ mm for normoxic and hypoxic cells, respectively.

We seek parameters of the model that give the experimentally observed values of distance that cells have migrated. The region of probable intersection between the two curves on the upper panel of Fig. 4 determines parameters $(t_{\rm diff},q)$ for normoxic cells; the respective region on the lower panel of Fig. 4 determines parameters $(t_{\rm diff},q)$ for hypoxic cells. Comparing the two regions in the parameter space, one can see that $t_{\rm diff}^{\rm norm} < t_{\rm diff}^{\rm hyp}$ and $q_{\rm norm} > q_{\rm hyp}$. The model suggests therefore that hypoxia not only suppresses cell motility (in contrast to our naive expectations), but it also substantially reduces the strength of cell-cell adhesion. We find this result to be quite important: The decreased cell-cell adhesion allows hypoxic cells to detach from the tumor much easier, which leads to an enhanced invasion, despite the decreased cell motility.

Theoretical modeling is successful when it not only describes the existing experimental observations, but also can produce an experimentally testable hypothesis. One of the main theoretical predictions of our model is that the strength of cell-cell adhesion decreases due to hypoxia. To test this hypothesis, we performed a Western blot to measure expression of E-cadherin, an important transmembrane protein that positively regulates the strength of cell-cell adhesion, for example, in carcinomas [22] and gliomas [23]. E-cadherin is known to act as an invasion suppressor molecule [22,23]. Our western blot experiments showed a clear down-regulation of E-cadherin 24 hours after cells had been placed under hypoxic conditions. This finding clearly confirms our theoretical prediction, and is consistent with a recent evidence that hypoxia down-regulates E-cadherin in breast cancer cells [24], see also [25]. Another important cell-cell adhesion molecule is N-cadherin, the expression of N-cadherin is known to correlate with the ability of cells to form aggregates [19]. We performed another experiment to study the effect of hypoxic conditions on the expression level of N-cadherins. Western blot showed a clear downregulation of N-cadherins, similarly to what was observed for E-cadherins. Thus, we verified that hypoxia down-regulates cadherin expression decreasing the strength of cell-cell adhesion.

IV. SUMMARY AND DISCUSSION

In summary, we demonstrated a successful application of a physically inspired approach to complex biological multicellular dynamics. Using discrete stochastic modeling, we explored the correspondence between the "microscopic" characteristics of a cell (cell diffusion coefficient, cell proliferation rate, and the strength of cell-cell adhesion) and the emerging macroscopic collective behavior of these cells. Specifically, we reproduced the experimental findings on migration of glioma cells under normoxic and hypoxic conditions in two different geometries and predicted a decrease both in cell

motility and in the strength of cell-cell adhesion due to hypoxia. We further confirmed the theoretical prediction on decrease of cell-cell adhesion in independent experiments. As we mentioned above, one can directly estimate the adhesion parameter q by measuring the shed rate of invasive cells from the tumor surface; this was done in Ref. [12]. It is known that cell-cell adhesion acts as a tissue surface tension [26], it would be interesting to find a relation between q and the surface tension of a tumor spheroid.

In this paper we investigated the effect of hypoxia employing discrete stochastic modeling. A promising approach in modeling biological systems is connecting the "microscopic" agent-based models and "macroscopic" continuum approach [5,27]. Let us consider the discrete model employed in the paper in case of zero adhesion, $q = 0$. Let us assume that the probability for proliferation is much smaller than the probability for migration. This is a reasonable biological assumption for glioma cells, since the typical time for migration is much smaller than the typical time for proliferation. In this case, the probability that the site n is occupied, $P(n)$, and the probability that the neighboring site $n+1$ (or the site $n-1$) is occupied, $P(n+1)$, are independent. Therefore, the master equation for cell dynamics (in one dimension) can be written in the form

$$\begin{aligned} P(n,m+1) - P(n,m) &= \frac{\bar{D}}{2}\{P(n-1,m)[1-P(n,m)]\} + \frac{\bar{D}}{2}\{P(n+1,m)[1-P(n,m)]\} - \frac{\bar{D}}{2}\{P(n,m)[1-P(n-1,m)]\} \\ &\quad - \frac{\bar{D}}{2}\{P(n,m)[1-P(n+1,m)]\} + \frac{\bar{\alpha}}{2}\{P(n-1,m)[1-P(n,m)]\} + \frac{\bar{\alpha}}{2}\{P(n+1,m)[1-P(n,m)]\} \\ &= \tfrac{1}{2}\{\bar{D} + \bar{\alpha}[1-P(n,m)]\} \times [P(n-1,m) - 2P(n,m) + P(n+1,m)] + \bar{\alpha}\, P(n,m)[1-P(n,m)], \end{aligned} \quad (3)$$

where $P(n,m)$ is the probability that the site n is occupied at a time step m, $\bar{D}$ is the probability to migrate to the empty neighboring site, and $\bar{\alpha}$ is the probability to proliferate to an empty neighboring site. Neglecting the contribution of proliferation to the diffusion term, we get the Fisher-Kolmogorov equation for $P(x,t)$ [and then Eq. (2) for the normalized density $u(x,t)$] in the continuum limit.

The situation for a nonzero adhesion parameter is more complicated. First, one can take a similar approach, writing down the master equation, see Ref. [28] for more detail. The resulting macroscopic equation is an elegant nonlinear diffusion equation. However, this procedure is valid only for small q, since for larger q, one cannot neglect correlations between the neighboring sites, and the probabilities $P(n,m)$ and $P(n+1,m)$ are not independent. It turns out that regime of large q is quite intriguing since the system may exhibit a phase transition, see Refs. [12,13]. Using the analogy with Ising model, we showed that the uniform system becomes unstable for $q > q_c$, which leads to cell clustering [12]. Carrying this analogy further, one can formulate a phenomenological equation, which describes cell dynamics for any value of q, and predicts a phase transition when q becomes larger than a critical threshold [27]. The equation is the modified Cahn-Hilliard equation with an extra proliferation term. In the limit of zero adhesion, this equation tends to the Fisher-Kolmogorov equation. The modified Cahn-Hilliard equation with an extra proliferation term can describe front propagation [27]. The propagating fronts are qualitatively similar to the Fisher-Kolmogorov fronts for $q < q_c$, but for $q > q_c$, a secondary density peak can be observed in the "tail" region, which represents cell clustering in the invasive zone [27]. There exist other (more complicated) models of Cahn-Hilliard type that incorporate the effects of cell-cell adhesion; see, for example, Ref. [29].

In this paper, we studied cell migration on a substrate. Although this *in vitro* setting allows investigation of the behavior of glioma cells (for example, various aspects of cell motility [30], cell spreading [31], or cell aggregation [12]), the real *in vivo* geometry is three dimensional. To mimic *in vivo* tumor growth, the dynamics of multicellular tumor spheroids in gel can be considered [11,19,32]. Investigation of cell invasion in these systems should take into account matrix degradation [33]. This is an interesting direction of future research.

The concept of emergence and emergent behavior in biological systems has become increasingly popular in recent years [1,34]. This concept addresses self-organization of complex biological systems and emphasizes the qualitative difference between the collective (macroscopic) behavior of a large number of microscopic agents and the behavior of individual agents. It is often claimed that complex biological systems are irreducible, and emergent macroscopic behavior cannot be predicted or deduced from the microscopic behavior [35]. Here we show that this is not always the case. In our model, the "microscopic" objects are individual glioma cells, 10–20 μm in diameter (this is actually a mesoscopic scale with respect to scales inside a cell). Using the model, we successfully predicted the collective cell behavior on a "macroscopic" scale, of the order of millimeters, formulating a minimalist model with relatively small number of parameters that nevertheless captures the essential physics and biology. The model provides a connection between the "microscopic" properties of individual cells (like the strength of cell-cell adhesion) and the "macroscopic" properties of the emergent system (like the velocity of propagation of cell density fronts). Importantly, the model provided theoretical predictions that were further tested in experiments. We demonstrated that employing minimalist models (where their formulation is possible) can substantially simplify the analysis and understanding of the emergent collective behavior of complex multicellular systems.

[1] T. S. Deisboeck and I. D. Couzin, BioEssays **31**, 190 (2009).
[2] P. Tracqui, Rep. Prog. Phys. **72**, 056701 (2009).
[3] G. Forgacs and S. A. Newman, *Biological Physics of the Developing Embryo* (Cambridge University Press, Cambridge, 2005).
[4] J. D. Murray, *Mathematical Biology. II. Spatial Models and Biomedical Applications*, 3rd ed. (Springer, New York, Berlin Heidelberg, 2003).
[5] M. J. Simpson, A. Merrifield, K. A. Landman, and B. D. Hughes, Phys. Rev. E **76**, 021918 (2007); C. Deroulers, M. Aubert, M. Badoual, and B. Grammaticos, *ibid.* **79**, 031917 (2009).
[6] E. C. Holland, Proc. Nat. Acad. Sci. USA **97**, 6242 (2000).
[7] CTBRUS, Central Brain Tumor Registry of the United States, Statistical Report, 1995-1999 (published 2002-2003).
[8] A. Giese, R. Bjerkvig, M. E. Berens, and M. Westphal, J. Clin. Oncol. **21**, 1624 (2003).
[9] S. Fedotov and A. Iomin, Phys. Rev. Lett. **98**, 118101 (2007).
[10] E. Khain, L. M. Sander, and A. Stein, Complexity **11**, 53 (2005); E. Khain and L. M. Sander, Phys. Rev. Lett. **96**, 188103 (2006).
[11] A. M. Stein, T. Demuth, D. Mobley, M. E. Berens, and L. M. Sander, Biophys. J. **92**, 356 (2007).
[12] E. Khain *et al.*, Europhys. Lett. **88**, 28006 (2009).
[13] E. Khain, L. M. Sander, and C. M. Schneider Mizell, J. Stat. Phys. **128**, 209 (2007).
[14] K. Huang, *Statistical Mechanics* (Wiley, New York, 1987).
[15] For example, S. Pennacchietti *et al.*, Cancer Cell **3**, 347 (2003); S. M. Evans *et al.*, Clin. Cancer Res. **10**, 8177 (2004); X. Zheng *et al.*, Cancer Sci. **98**, 674 (2007).
[16] For example, D. Dingli *et al.*, Math. Biosci. **199**, 55 (2006).
[17] P. K. Maini, D. L. S. McElwain, and D. Leavesley, Appl. Math. Lett. **17**, 575 (2004).
[18] M. J. Simpson, K. A. Landman, B. D. Hughes, and A. E. Fernando, Physica A **389**, 1412 (2010); A. E. Fernando, K. A. Landman, and M. J. Simpson, Phys. Rev. E **81**, 011903 (2010); P. Gerlee and A. R. A. Anderson, J. Theor. Biol. **259**, 67 (2009); G. Y. Ouaknin and P. Z. Bar-Yoseph, Biophys. J. **97**, 1811 (2009).
[19] B. Hegedus *et al.*, Biophys. J. **91**, 2708 (2006).
[20] M. H. Zaman *et al.*, Proc. Nat. Acad. Sci. **103**, 10889 (2006).
[21] In experiments, increase in cell-substrate adhesion may either increase or decrease the motility of cells, depending on functional ligand and receptor density [20].
[22] K. Vleminckx *et al.*, Cell **66**, 107 (1991).
[23] Q. H. Meng *et al.*, Acta Pharmacol. Sin. **26**, 492 (2005).
[24] J. Chen, N. Imanaka, J. Chen, and J. D. Griffin, Br. J. Cancer **102**, 351 (2010).
[25] N. J. Popawski *et al.*, Bull. Math. Biol. **71**, 1189 (2009).
[26] C. Norotte *et al.*, Europhys. Lett. **81**, 46003 (2008).
[27] E. Khain and L. M. Sander, Phys. Rev. E **77**, 051129 (2008).
[28] M. J. Simpson, C. Towne, D. L. S. McElwain, and Z. Upton, Phys. Rev. E **82**, 041901 (2010).
[29] V. Cristini, X. R. Li, J. S. Lowengrub, and S. M. Wise, J. Math. Biol. **58**, 723 (2009).
[30] T. Demuth *et al.*, Clin. Exp. Metastasis **18**, 589 (2001); D. Selmeczi *et al.*, Biophys. J. **89**, 912 (2005); B. Hegedus *et al.*, J. Neuro-oncol. **67**, 147 (2004).
[31] P. L. Ryan *et al.*, Proc. Nat. Acad. Sci. **98**, 4323 (2001).
[32] R. M. Sutherland, Science **240**, 177 (1988); T. S. Deisboeck *et al.*, Cell Proliferation **34**, 115 (2001); L. M. Sander and T. S. Deisboeck, Phys. Rev. E **66**, 051901 (2002); Y. Kim, M. A. Stolarska, and H. G. Othmer, Math. Mod. Methods Appl. Sci. **17**, 1773 (2007); B. M. Rubenstein and L. J. Kaufman, Biophys. J. **95**, 5661 (2008); K. Pham *et al.*, J. R. Soc. Interface **8**, 16 (2011).
[33] P. Macklin *et al.*, J. Math. Biol. **58**, 765 (2009).
[34] R. B. Laughlin, *A Different Universe: Reinventing Physics from the Bottom Down* (Basic Books, New York, 2005).
[35] R. B. Laughlin and D. Pines, Proc. Nat. Acad. Sci. **97**, 28 (2000); M. H. V. Van Regenmortel, EMBO Rep. **5**, 1016 (2004).